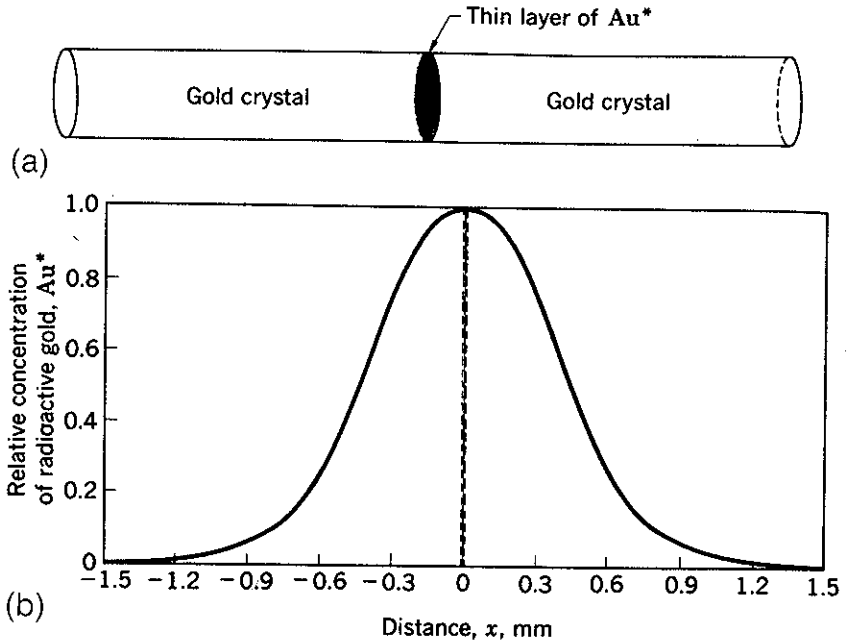

Fig. 2.14 Illustration of the principle of tracer diffusion and of the planar source method for determining the self-diffusion coefficient of gold. (a) Initial diffusion couple with planar source of radioactive gold Au*. (b) Distribution of Au* after diffusion for 100 h at 920 °C. (After A.G. Guy, *Introduction to Materials Science*, McGraw-Hill, New York, 1971.)

This shows in fact that D_v is many orders of magnitude greater than D_A the diffusivity of substitutional atoms.

2.3.3 *Diffusion in Substitutional Alloys*

During self-diffusion all atoms are chemically identical. Thus the probability of finding a vacancy adjacent to any atom and the probability that the atom will make a jump into the vacancy is equal for all atoms. This leads to a simple relationship between jump frequency and diffusion coefficient. In binary substitutional *alloys*, however, the situation is more complex. In general, the rate at which solvent (A) and solute (B) atoms can move into a vacant site is not equal and each atomic species must be given its own *intrinsic* diffusion coefficient D_A or D_B.

The fact that the A and B atoms occupy the same sites has important consequences on the form that Fick's first and second laws assume for substitutional alloys. It will be seen later that when the A and B atoms jump at different rates the presence of concentration gradients induces a movement of the lattice through which the A and B atoms are diffusing.

D_A and D_B are defined such that Fick's first law applies to diffusion *relative to the lattice*, that is

$$J_A = -D_A \frac{\partial C_A}{\partial x} \tag{2.39}$$

$$J_B = -D_B \frac{\partial C_B}{\partial x} \tag{2.40}$$

where J_A and J_B are the fluxes of A and B atoms *across a given lattice plane*. This point did not need emphasizing in the case of interstitial diffusion because the lattice planes of the parent atoms were unaffected by the diffusion process. It will be seen, however, that the situation is different in the case of substitutional diffusion.

In order to derive Fick's second law let us consider the interdiffusion of A and B atoms in a diffusion couple that is made by welding together blocks of pure A and B as shown in Fig. 2.15a. If the couple is annealed at a high enough temperature, a concentration profile will develop as shown.

If we make the simplifying assumption that the total number of atoms per unit volume is a constant, C_0, independent of composition, then

$$C_0 = C_A + C_B \tag{2.41}$$

and

$$\frac{\partial C_A}{\partial x} = -\frac{\partial C_B}{\partial x} \tag{2.42}$$

Hence at a given position the concentration gradients driving the diffusion of A and B atoms are equal but opposite, and the fluxes of A and B *relative to the lattice* can be written as

$$J_A = -D_A \frac{\partial C_A}{\partial x} \tag{2.43}$$

$$J_B = D_B \frac{\partial C_A}{\partial x}$$

These fluxes are shown schematically in Fig. 2.15 for the case $D_A > D_B$, i.e. $|J_A| > |J_B|$.

When atoms migrate by the vacancy process the jumping of an atom into a vacant site can equally well be regarded as the jumping of the vacancy onto the atom, as illustrated in Fig. 2.16. In other words, if there is a net flux of atoms in one direction there is an equal flux of vacancies in the opposite direction. Thus in Fig. 2.15a there is a flux of vacancies $-J_A$ due to the migration of a A atoms *plus* a flux of vacancies $-J_B$ due to the diffusion of B atoms. As $J_A > J_B$ there will be a net flux of vacancies

$$J_v = -J_A - J_B \tag{2.44}$$

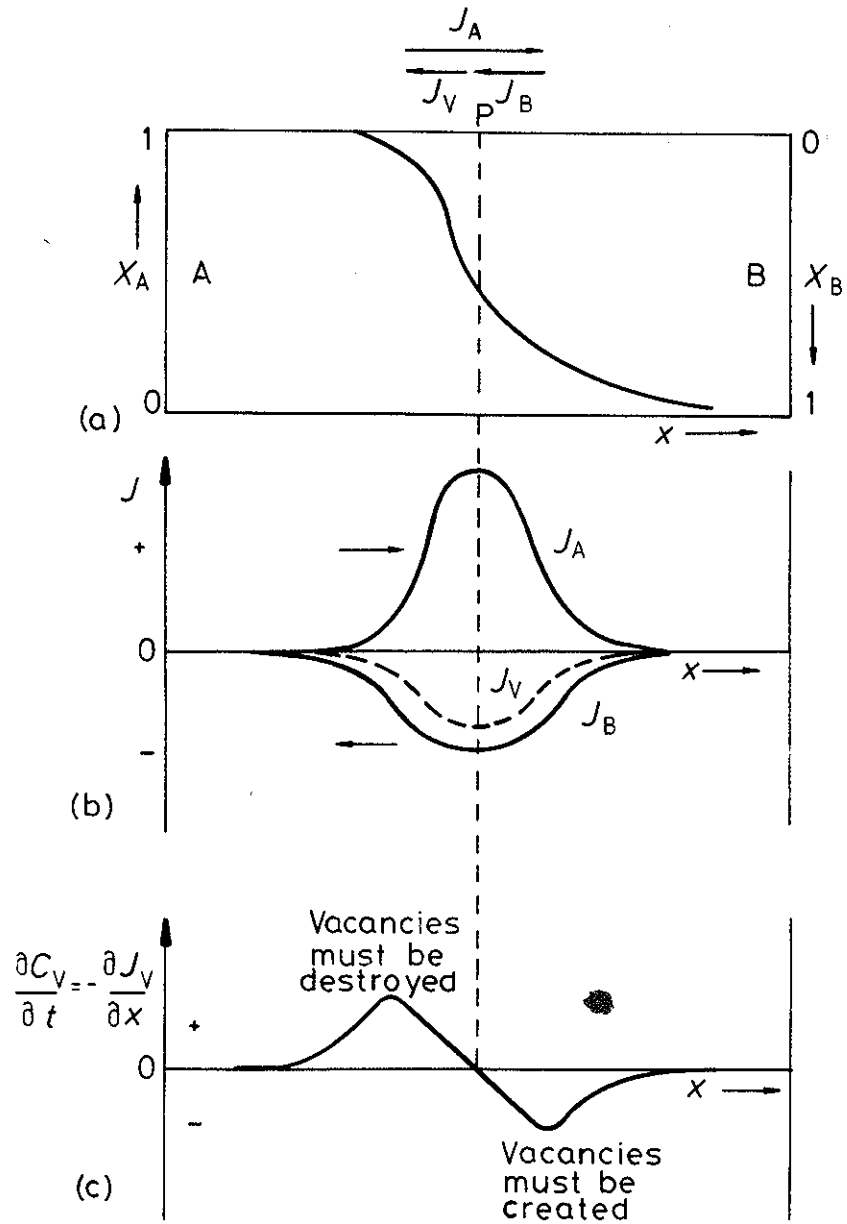

Fig. 2.15 Interdiffusion and vacancy flow. (a) Composition profile after interdiffusion of A and B. (b) The corresponding fluxes of atoms and vacancies as a function of position x. (c) The rate at which the vacancy concentration would increase or decrease if vacancies were not created or destroyed by dislocation climb.

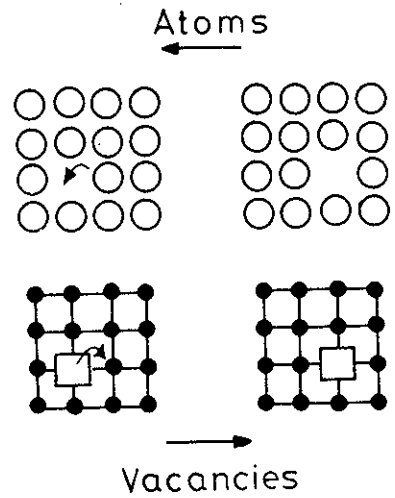

Fig. 2.16 The jumping of atoms in one direction can be considered as the jumping of vacancies in the other direction.

This is indicated in vector notation in Fig. 2.15a. In terms of D_A and D_B, therefore

$$J_v = (D_A - D_B)\frac{\partial C_A}{\partial x} \tag{2.45}$$

This leads to a variation in J_v across the diffusion couple as illustrated in Fig. 2.15b.

In order to maintain the vacancy concentration everywhere near equilibrium vacancies must be created on the B-rich side and destroyed on the A-rich side. The rate at which vacancies are *created* or *destroyed* at any point is given by $\partial C_v/\partial t = -\partial J_v/\partial x$ (Equation 2.16) and this varies across the diffusion couple as shown in Fig. 2.15c.

It is the net flux of vacancies across the middle of the diffusion couple that gives rise to movement of the lattice. Jogged edge dislocations can provide a convenient source or sink for vacancies as shown in Fig. 2.17. Vacancies can be absorbed by the extra half-plane of the edge dislocation shrinking while growth of the plane can occur by the emission of vacancies. If this or a similar mechanism operates on each side of the diffusion couple then the required flux of vacancies can be generated as illustrated in Fig. 2.18. This means that extra atomic planes will be introduced on the B-rich side while whole planes of atoms will be 'eaten' away on the A-rich side. Consequently the lattice planes in the middle of the couple will be shifted to the left.

The velocity at which any given lattice plane moves, v, can be related to the flux of vacancies crossing it. If the plane has an area A, during a small time interval δt, the plane will sweep out a volume of $Av \cdot \delta t$ containing $Av \cdot \delta t \cdot C_0$ atoms. This number of atoms is removed by the total number of vacancies crossing the plane in the same time interval, i.e. $J_v A \cdot \delta t$, giving

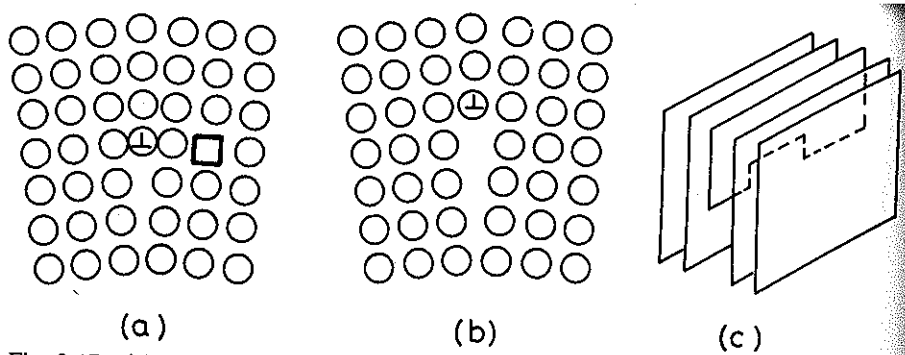

Fig. 2.17 (a) before, (b) after: a vacancy is absorbed at a jog on an edge dislocation (positive climb). (b) before, (a) after: a vacancy is created by negative climb of an edge dislocation. (c) Perspective drawing of a jogged edge dislocation.

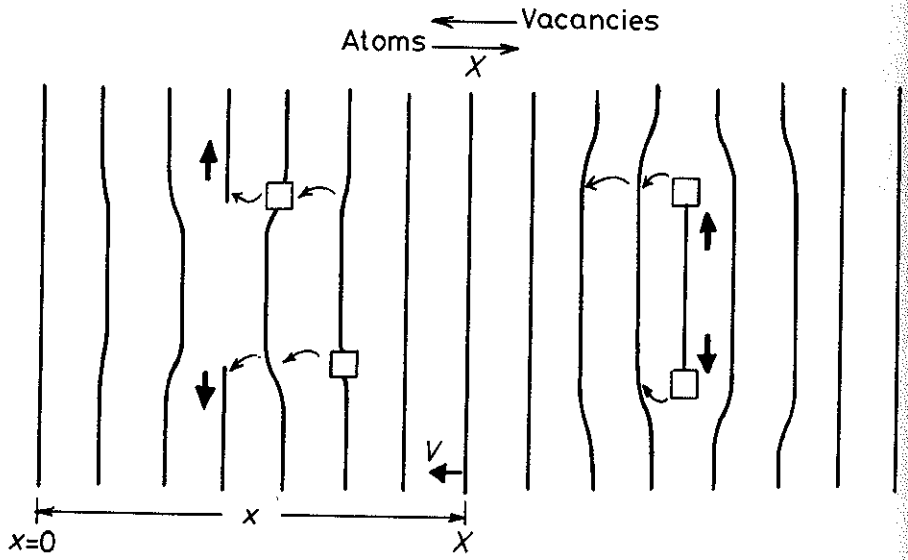

Fig. 2.18 A flux of vacancies causes the atomic planes to move through the specimen.

$$J_v = C_0 v \tag{2.46}$$

Thus the velocity of the lattice planes will vary across the couple in the same way as J_v, see Fig. 2.15b. Substituting Equation 2.45 gives

$$v = (D_A - D_B)\frac{\partial X_A}{\partial x} \tag{2.47}$$

where the mole fraction of A, $X_A = C_A/C_0$

In practice, of course, internal movements of lattice planes are usually not directly of interest. More practical questions concern how long homogenization of an alloy takes, or how rapidly the composition will change at a fixed position relative to the ends of a specimen. To answer these questions we can derive Fick's second law for substitutional alloys.

Consider a thin slice of material δx thick at a *fixed distance x from one end of the couple* which is outside the diffusion zone as shown in Fig. 2.19. If the *total* flux of A atoms entering this slice across plane 1 is J'_A and the *total* flux leaving is $J'_A + (\partial J'_A/\partial x)\delta x$ the same arguments as were used to derive Equation 2.16 can be used to show that

$$\frac{\partial C_A}{\partial t} = -\frac{\partial J'_A}{\partial x} \tag{2.48}$$

The total flux of A atoms across a stationary plane with respect to the *specimen* is the sum of two contributions: (i) a diffusive flux $J_A = -D_A\,\partial C_A/\partial x$ due to diffusion relative to the *lattice*, and (ii) a flux $v \cdot C_A$ due to the velocity of the lattice in which diffusion is occurring. Therefore:

$$J'_A = -D_A\frac{\partial C_A}{\partial x} + vC_A \tag{2.49}$$

By combining this equation with Equation 2.47 we obtain the equivalent of Fick's first law for the flux relative to the specimen ends:

$$J'_A = -(X_B D_A + X_A D_B)\frac{\partial C_A}{\partial x} \tag{2.50}$$

where $X_A = C_A/C_0$ and $X_B = C_B/C_0$ are the mole fractions of A and B respectively. This can be simplified by defining an *interdiffusion coefficient* $\tilde{D}$ as

$$\tilde{D} = X_B D_A + X_A D_B \tag{2.51}$$

so that Fick's first law becomes

$$J'_A = -\tilde{D}\frac{\partial C_A}{\partial x} \tag{2.52}$$

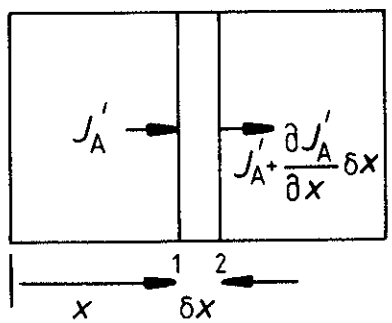

Fig. 2.19 Derivation of Fick's second law for interdiffusion. (See text for details.)

Likewise,

$$J'_B = -\tilde{D}\frac{\partial C_B}{\partial x} = \tilde{D}\frac{\partial C_A}{\partial x}$$

i.e.

$$J'_B = -J'_A$$

Substitution of Equation 2.52 into Equation 2.48 gives

$$\frac{\partial C_A}{\partial t} = \frac{\partial}{\partial x}\left(\tilde{D}\,\frac{\partial C_A}{\partial x}\right) \tag{2.53}$$

This equation is Fick's second law for diffusion in substitutional alloys. The only difference between this equation and Equation 2.18 (for interstitial diffusion) is that the *interdiffusion* coefficient D for substitutional alloys depends on D_A and D_B whereas in interstitial diffusion D_B alone is needed. Equations 2.47 and 2.51 were first derived by Darken[5] and are usually known as *Darken's equations*.

By solving Equation 2.53 with appropriate boundary conditions it is possible to obtain $C_A(x, t)$ and $C_B(x, t)$, i.e. the concentration of A and B at any position (x) after any given annealing time (t). The solutions that were given in Section 2.2.5 will be applicable to substitutional alloys provided the range of compositions is small enough that any effect of composition on $\tilde{D}$ can be ignored. For example, if $\tilde{D}$ is known the characteristic relaxation time for an homogenization anneal would be given by Equation 2.21 using $\tilde{D}$ in place of D_B, i.e.

$$\tau = \frac{l^2}{\pi^2\tilde{D}} \tag{2.54}$$

If the initial composition differences are so great that changes in $\tilde{D}$ become important then more complex solutions to Equation 2.53 must be used. These will not be dealt with here, however, as they only add mathematical complexities without increasing our understanding of the basic principles[6].

Experimentally it is possible to measure $\tilde{D}$ by determining the variation of X_A or X_B after annealing a diffusion couple for a given time such as that shown in Fig. 2.15a. In cases where $\tilde{D}$ can be assumed constant a comparison of Equation 2.26 and the measured concentration profile would give $\tilde{D}$. When $\tilde{D}$ is not constant there are graphical solutions to Fick's second law that enable $\tilde{D}$ to be determined at any composition. In order to determine D_A and D_B separately it is also necessary to measure the velocity of the lattice at a given point in the couple. This can be achieved in practice by inserting insoluble wires at the interface before welding the two blocks together. These wires remain in effect 'fixed' to the lattice planes and their displacement after a given annealing time can be used to calculate v. When v and $\tilde{D}$ are known, Equations 2.47 and 2.51 can be used to calculate D_A and D_B for the composition at the markers.

The displacement of inert wires during diffusion was first observed by

Smigelskas and Kirkendall in 1947[7] and is usually known as the *Kirkendall effect*. In this experiment a block of α-brass (Cu–30wt% Zn) was wound with molybdenum wire and encapsuled in a block of pure Cu, as shown in Fig. 2.20. After annealing at a high temperature it was found that the separation of the markers (w) had decreased. This is because $D_{Zn} > D_{Cu}$ and the zinc atoms diffuse out of the central block faster than they are replaced by copper atoms diffusing in the opposite direction. Similar effects have since been demonstrated in many other alloy systems. In general it is found that in any given couple, atoms with the lower melting point possess a higher D. The exact value of D, however, varies with the composition of the alloy. Thus in Cu–Ni alloys D_{Cu}, D_{Ni} and $\tilde{D}$ are all composition dependent, increasing as X_{Cu} increases, Fig. 2.21.

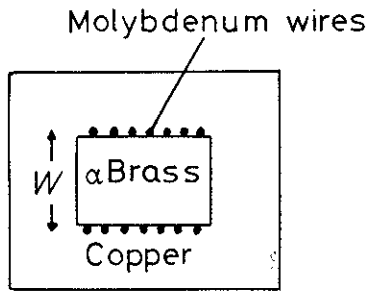

Fig. 2.20 An experimental arrangement to show the Kirkendall effect.

In Fig. 2.17 it was assumed that the extra half-planes of atoms that grew or shrank due to the addition or loss of atoms, were parallel to the original weld interface so that there were no constraints on the resultant local expansion or contraction of the lattice. In practice, however, these planes can be oriented in many directions and the lattice will also try to expand or contract parallel to the weld interface. Such volume changes are restricted by the surrounding material with the result that two-dimensional compressive stresses develop in regions where vacancies are created, while tensile stresses arise in regions where vacancies are destroyed. These stress fields can even induce plastic deformation resulting in microstructures characteristic of hot deformation.

Vacancies are not necessarily all annihilated at dislocations, but can also be absorbed by internal boundaries and free surfaces. However, those not absorbed at dislocations mainly agglomerate to form holes or voids in the lattice. Void nucleation is difficult because it requires the creation of a new surface and it is generally believed that voids are heterogeneously nucleated at impurity particles. The tensile stresses that arise in conjunction with vacancy destruction can also play a role in the nucleation of voids. When voids are formed the equations derived above cannot be used without modification.

In concentrated alloys the experimentally determined values of $\tilde{D}$, D_A and D_B are also found to show the same form of temperature dependence as all

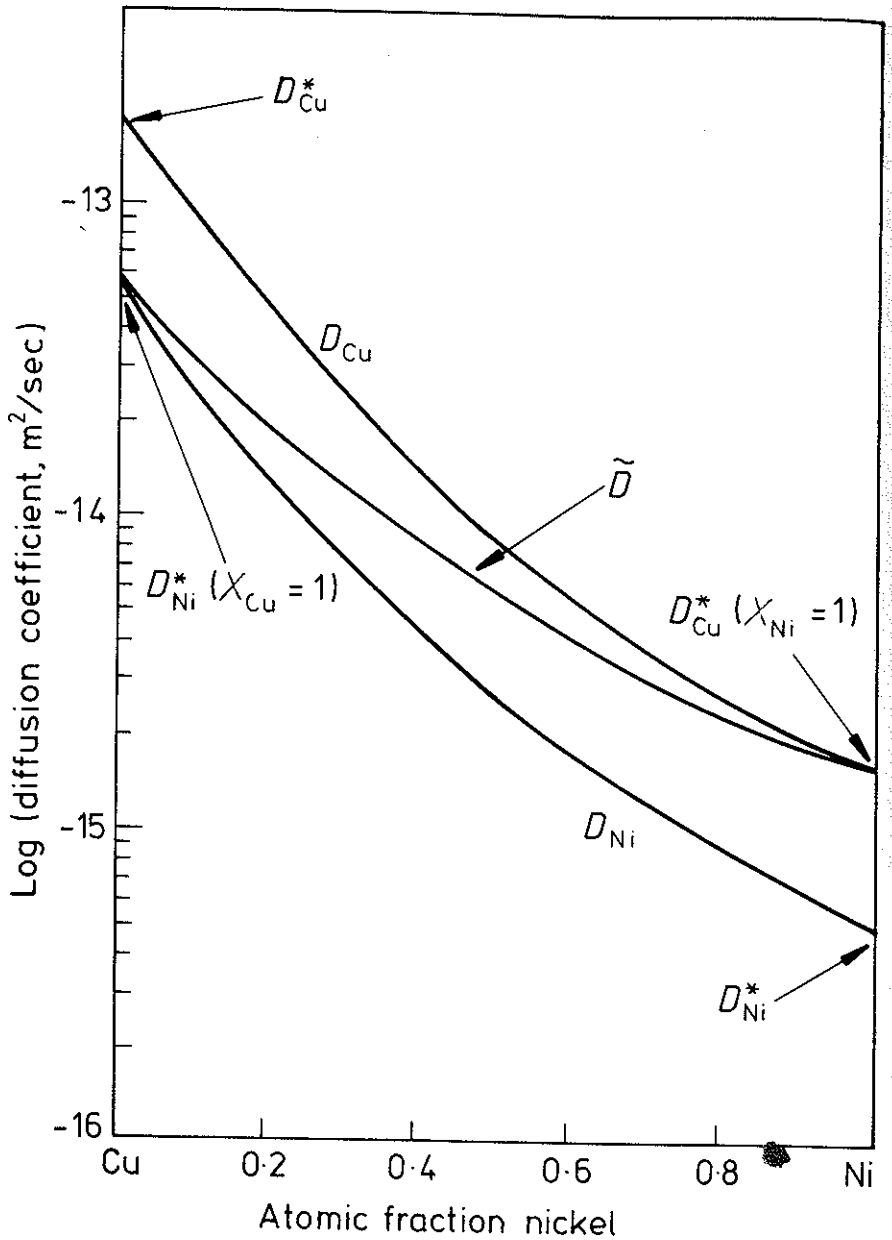

Fig. 2.21 The relationship between the various diffusion coefficients in the Cu–Ni system at 1000 °C (After A.G. Guy, *Introduction to Materials Science*, McGraw-Hill, New York, 1971.)

other diffusivities, so that

$$\tilde{D} = \tilde{D}_0 \exp \frac{-Q}{RT} \tag{2.55}$$

$$D_A = D_{A0} \exp \frac{-Q_A}{RT} \tag{2.56}$$

$$D_B = D_{B0} \exp \frac{-Q_B}{RT} \tag{2.57}$$

However the factors that determine D_0 and Q in these cases are uncertain and there is no simple atomistic model for concentrated solutions.

The variation of $\tilde{D}$ with composition can be estimated in cases where it has not been measured, by utilizing two experimental observations[8]:

1. For a given crystal structure, $\tilde{D}$ at the melting point is roughly constant. Therefore if adding B to A decreases the melting point, $\tilde{D}$ will increase, at a given temperature, and vice versa.
2. For a given solvent and temperature, both interstitial and substitutional diffusion are more rapid in a bcc lattice than a close-packed lattice. For example, for the diffusion of carbon in Fe at 910 °C, $D_c^\alpha/D_c^\gamma \sim 100$. At 850 °C the self-diffusion coefficients for Fe are such that $D_{Fe}^\alpha/D_{Fe}^\gamma \sim 100$. The reason for this difference lies in the fact that the bcc structure is more open and the diffusion processes require less lattice distortion.

2.3.4 *Diffusion in Dilute Substitutional Alloys*

Another special situation arises with diffusion in dilute alloys. When $X_B \sim 0$ and $X_A \sim 1$, Equation 2.51 becomes

$$\tilde{D} = D_B \tag{2.58}$$

This is reasonable since it means that the rate of homogenization in dilute alloys is controlled by how fast the solute (B) atoms can diffuse. Indeed the only way homogenization can be achieved is by the migration of the B atoms into the solute-depleted regions. D_B for a dilute solution of B in A is called the impurity diffusion coefficient. Such data is more readily available than interdiffusion data in concentrated alloys. One way in which impurity diffusion coefficients can be measured is by using radioactive tracers.

It is often found that D_B in a dilute solution of B in A is greater than D_A. The reason for this is that the solute atoms can attract vacancies so that there is *more* than a random probability of finding a vacancy next to a solute atom with the result that they can diffuse faster than the solvent. An attraction between a solute atom and a vacancy can arise if the solute atom is larger than the solvent atoms or if it has higher valency. If the binding energy is very large the vacancy will be unable to'escape' from the solute atom. In this case the solute–vacancy pair can diffuse through the lattice together.

2.4 Atomic Mobility

Fick's first law is based on the assumption that diffusion eventually stops, that is equilibrium is reached, when the concentration is the same everywhere. Strictly speaking this situation is never true in practice because real materials always contain lattice defects such as grain boundaries, phase boundaries and dislocations. Some atoms can lower their free energies if they migrate to such defects and at 'equilibrium' their concentrations will be higher in the vicinity of the defect than in the matrix. Diffusion in the vicinity of these defects is therefore affected by both the concentration gradient and the gradient of the interaction energy. Fick's law alone is insufficient to describe how the concentration will vary with distance and time.

As an example consider the case of a solute atom that is too big or too small in comparison to the space available in the solvent lattice. The potential energy of the atom will then be relatively high due to the strain in the surrounding matrix. However, this strain energy can be reduced if the atom is located in a position where it better matches the space available, e.g. near dislocations and in boundaries, where the matrix is already distorted.

Segregation of atoms to grain boundaries, interfaces and dislocations is of great technological importance. For example the diffusion of carbon or nitrogen to dislocations in mild steel is responsible for strain ageing and blue brittleness. The segregation of impurities such as Sb, Sn, P and As to grain boundaries in low-alloy steels produces temper embrittlement. Segregation to grain boundaries affects the mobility of the boundary and has pronounced effects on recrystallization, texture and grain growth. Similarly the rate at which phase transformations occur is sensitive to segregation at dislocations and interfaces.

The problem of atom migration can be solved by considering the thermodynamic condition for equilibrium; namely that the chemical potential of an atom must be the same everywhere. Diffusion continues in fact until this condition is satisfied. Therefore it seems reasonable to suppose that in general the flux of atoms at any point in the lattice is proportional to the chemical potential gradient. Fick's first law is merely a special case of this more general approach.

An alternative way to describe a flux of atoms is to consider a net *drift* velocity (v) superimposed on the random jumping motion of each diffusing atom. The drift velocity is simply related to the diffusive flux via the equation

$$J_B = v_B C_B \tag{2.59}$$

Since atoms always migrate so as to remove differences in chemical potential it is reasonable to suppose that the drift velocity is proportional to the local chemical potential gradient, i.e.

$$v_B = -M_B \frac{\partial \mu_B}{\partial x} \tag{2.60}$$

where M_B is a constant of proportionality known as the atomic mobility. Since μ_B has units of energy the derivative of μ_B with respect to distance ($\partial \mu_B / \partial x$) is effectively the chemical 'force' causing the atom to migrate.

Combining Equations 2.59 and 2.60 gives

$$J_B = -M_B C_B \frac{\partial \mu_B}{\partial x} \tag{2.61}$$

Intuitively it seems that the mobility of an atom and its diffusion coefficient must be closely related. The relationship can be obtained by relating $\partial \mu / \partial x$ to $\partial C / \partial x$ for a stress-free solid solution. Using Equation 1.70 and $C_B = X_B / V_m$ Equation 2.61 becomes

$$J_B = -M_B \frac{X_B}{V_m} \cdot \frac{RT}{X_B} \left\{ 1 + \frac{\mathrm{d} \ln \gamma_B}{\mathrm{d} \ln X_B} \right\} \frac{\partial X_B}{\partial x} \tag{2.62}$$

i.e.

$$J_B = -M_B RT \left\{ 1 + \frac{\mathrm{d} \ln \gamma_B}{\mathrm{d} \ln X_B} \right\} \frac{\partial C_B}{\partial x} \tag{2.63}$$

Comparison with Fick's first law gives the required relationship:

$$D_B = M_B RT \left\{ 1 + \frac{\mathrm{d} \ln \gamma_B}{\mathrm{d} \ln X_B} \right\} \tag{2.64}$$

Similarly

$$D_A = M_A RT \left\{ 1 + \frac{\mathrm{d} \ln \gamma_A}{\mathrm{d} \ln X_A} \right\} \tag{2.65}$$

For *ideal* or *dilute* solutions ($X_B \to 0$)γ_B is a constant and the term in brackets is unity, i.e.

$$D_B = M_B RT \tag{2.66}$$

For non-ideal concentrated solutions the terms in brackets, the so-called thermodynamic factor, must be included. As shown by Equation 1.71 this factor is the same for both A and B and is simply related to the curvature of the molar free energy–composition curve.

When diffusion occurs in the presence of a strain energy gradient, for example, the expression for the chemical potential can be modified to include the effect of an elastic strain energy term E which depends on the position (x) relative to a dislocation, say

$$\mu_B = G_B + RT \ln \gamma_B X_B + E \tag{2.67}$$

Following the above procedure, this gives

$$J_B = -D_B \cdot \frac{\partial C_B}{\partial x} - \frac{D_B C_B}{RT} \cdot \frac{\partial E}{\partial x} \tag{2.68}$$

It can thus be seen that in addition to the effect of the concentration gradient the diffusive flux is also affected by the gradient of strain energy, $\partial E/\partial x$.

Other examples of atoms diffusing towards regions of high concentration can be found when diffusion occurs in the presence of an electric field or a temperature gradient. These are known as electromigration and thermomigration respectively[9]. Cases encountered in phase transformations can be found where atoms migrate across phase boundaries, or, as mentioned in the introduction, when the free energy curve has a negative curvature. The latter is known as spinodal decomposition.

2.5 Tracer Diffusion in Binary Alloys

The use of radioactive tracers were described in connection with self-diffusion in pure metals. It is, however, possible to use radioactive tracers to determine the intrinsic diffusion coefficients of the components in an alloy. The method is similar to that shown in Fig 2.14 except that a small quantity of a suitable radioactive tracer, e.g. B*, is allowed to diffuse into a homogeneous bar of A/B solution. The value obtained for D from Equation 2.35 is the tracer diffusion coefficient D_B^*.

Such experiments have been carried out on a whole series of gold-nickel alloys at 900 °C[10]. At this temperature gold and nickel are completely soluble in each other, Fig. 2.22a. The results are shown in Fig. 2.22c. Since radioactive isotopes are chemically identical it might appear at first sight that the tracer diffusivities (D_{Au}^* and D_{Ni}^*) should be identical to the intrinsic diffusivities (D_{Au} and D_{Ni}) determined by marker movement in a diffusion couple. This would be convenient as the intrinsic diffusivities are of more practical value whereas it is much easier to determine tracer diffusities. However, it can be demonstrated that this is not the case. D_{Au}^* gives the rate at which Au* (or Au) atoms diffuse in a *chemically homogeneous* alloy, whereas D_{Au} gives the diffusion rate of Au when a concentration gradient is present.

The Au–Ni phase diagram contains a miscibility gap at low temperatures implying that $\Delta H_{mix} > 0$ (the gold and nickel atoms 'dislike' each other). Therefore, whereas the jumps made by Au atoms in a chemically homogeneous alloy will be equally probable in all directions, in a concentration gradient they will be biased away from the Ni-rich regions. The rate of homogenization will therefore be slower in the second case, i.e. $D_{Au} < D_{Au}^*$ and $D_{Ni} < D_{Ni}^*$. On the other hand since the chemical potential gradient is the driving force for diffusion in both types of experiment it is reasonable to suppose that the atomic mobilities are not affected by the concentration gradient. If this is true the intrinsic chemical diffusivities and tracer diffusivities can be related as follows.

In the tracer diffusion experiment the tracer essentially forms a dilute solution in the alloy. Therefore from Equation 2.66

$$D_B^* = M_B^* RT = M_B RT \tag{2.69}$$

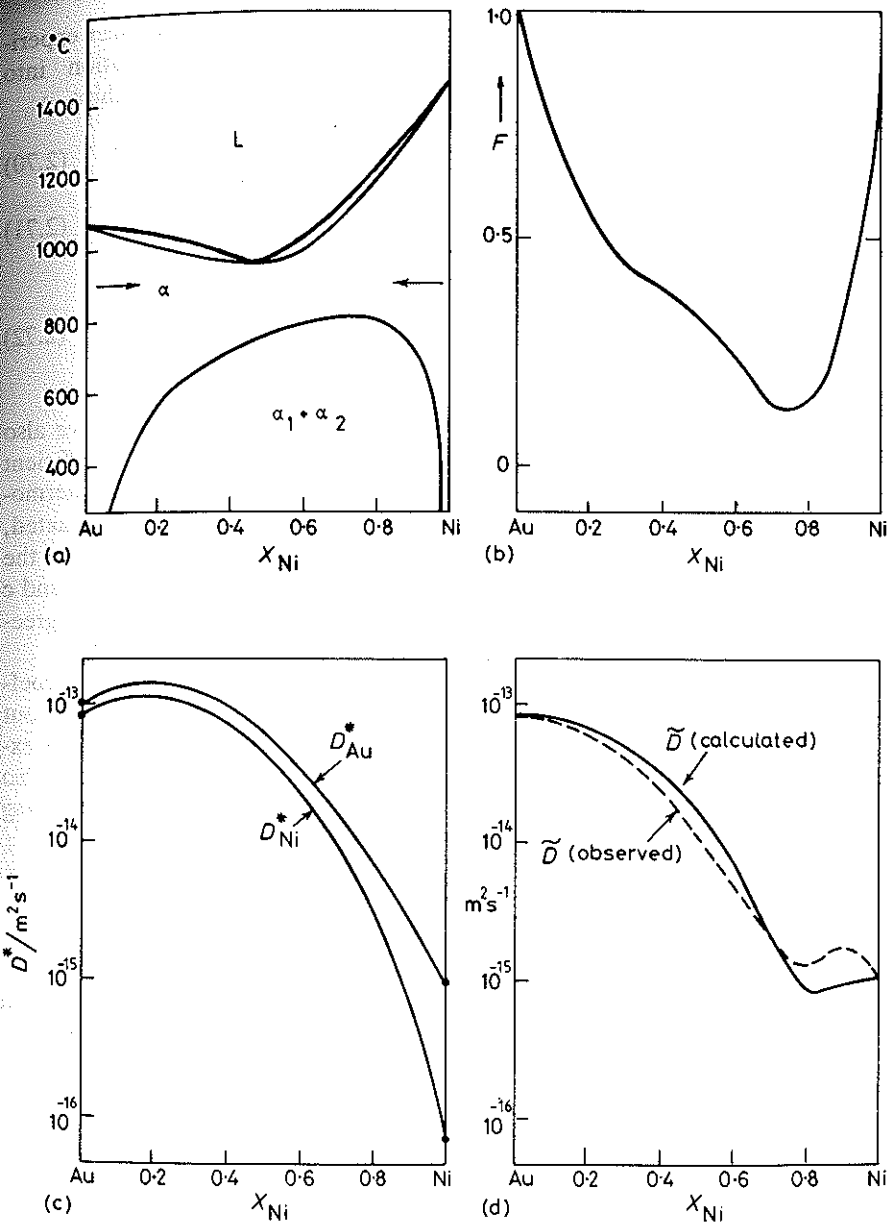

Fig. 2.22 Interdiffusion in Au–Ni alloys at 900 °C (a) Au–Ni phase diagram, (b) the thermodynamic factor, F, at 900 °C, (c) experimentally measured tracer diffusivities at 900 °C, (d) experimentally measured interdiffusion coefficients compared with values calculated from (b) and (c). (From J.E. Reynolds, B.L. Averbach and Morris Cohen, *Acta Metallurgica*, **5** (1957) 29.)

The second equality has been obtained by assuming M_B^* in the tracer experiment equals M_B in the chemical diffusion case. Substitution into Equations 2.64 and 2.51 therefore leads to the following relationships

$$D_A = FD_A^*$$
$$D_B = FD_B^* \tag{2.70}$$

and $$\tilde{D} = F(X_B D_A^* + X_A D_B^*) \tag{2.71}$$

where F is the thermodynamic factor, i.e.

$$F = \left\{1 + \frac{\mathrm{d} \ln \gamma_A}{\mathrm{d} \ln X_A}\right\} = \left\{1 + \frac{\mathrm{d} \ln \gamma_B}{\mathrm{d} \ln X_B}\right\} = \frac{X_A X_B}{RT} \frac{\mathrm{d}^2 G}{\mathrm{d}X^2} \tag{2.72}$$

The last equality follows from Equation 1.71.

In the case of the Au-Ni system, diffusion couple experiments have also been carried out so that data are available for the interdiffusion coefficient $\tilde{D}$, the full line in Fig. 2.22d. In addition there is also enough thermodynamic data on this system for the thermodynamic factor F to be evaluated, Fig. 2.22b. It is therefore possible to check the assumption leading to the second equality in Equation 2.69 by combining the data in Fig. 2.22b and c using Equation 2.71. This produces the solid line in Fig. 2.22d. The agreement is within experimental error.

Before leaving Fig. 2.22 it is interesting to note how the diffusion coefficients are strongly composition dependent. There is a difference of about three orders of magnitude across the composition range. This can be explained by the lower liquidus temperature of the Au-rich compositions. Also in agreement with the rules of thumb given earlier, Au, with the lower melting temperature, diffuses faster than Ni at all compositions.

2.6 Diffusion in Ternary Alloys

The addition of a third diffusing species to a solid solution produces mathematical complexities which will not be considered here. Instead let us consider an illustrative example of some of the additional effects that can arise. Fe–Si–C alloys are particularly instructive for two reasons. Firstly silicon raises the chemical potential (or activity) of carbon in solution, i.e. carbon will not only diffuse from regions of high carbon concentration but also from regions rich in silicon. Secondly the mobilities of carbon and silicon are widely different. Carbon, being an interstitial solute, is able to diffuse far more rapidly than the substitutionally dissolved silicon.

Consider two pieces of steel, one containing 3.8% silicon and 0.48% carbon and the other 0.44% carbon but no silicon. If the two pieces are welded together and austenitized at 1050 °C, the carbon concentration profile shown in Fig. 2.23b is produced. The initial concentrations of silicon and carbon in the couple are shown in Fig. 2.23a and the resultant chemical potentials of carbon by the dotted line in Fig. 2.23c. Therefore carbon atoms

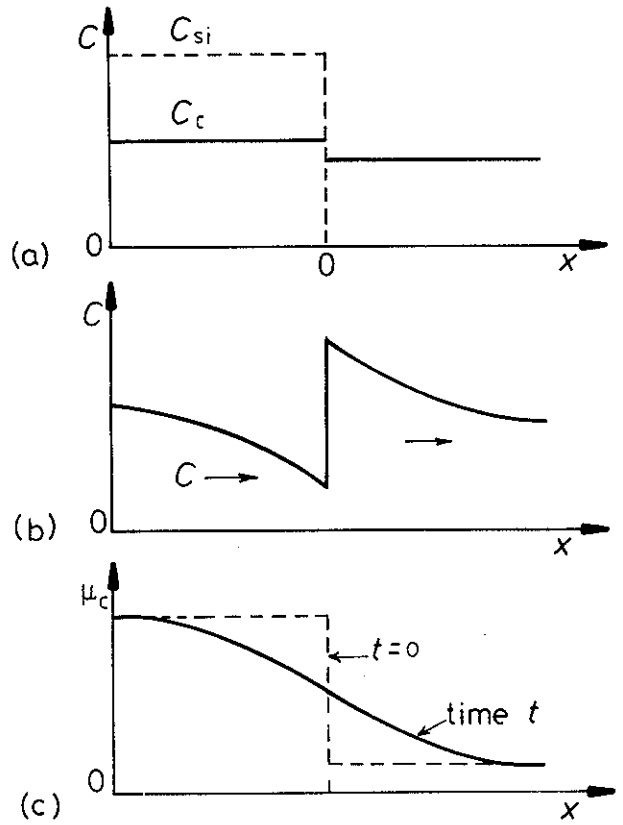

Fig. 2.23 (a) Carbon and silicon distribution in iron at $t = 0$. (b) Carbon distribution after high-temperature anneal. (c) Chemical potential of carbon v. distance.

on the silicon-rich side will jump over to the silicon-free side until the difference in concentration at the interface is sufficient to equalize the activity, or chemical potential, of carbon on both sides. The carbon atoms at the interface are therefore in *local equilibrium* and the interfacial compositions remain constant as long as the silicon atoms do not migrate. Within each half of the couple the silicon concentration is initially uniform and the carbon atoms diffuse down the concentration gradients as shown in Fig. 2.23b. The resultant chemical potential varies smoothly across the whole specimen Fig. 2.23c. If the total length of the diffusion couple is sufficiently small the carbon concentration in each block will eventually equal the interfacial compositions and the chemical potential of carbon will be the same everywhere. The alloy is now in a state of partial equilibrium. It is only partial because the chemical potential of the silicon is not uniform. Given sufficient time the silicon atoms will also diffuse over significant distances and the carbon atoms will continually redistribute themselves to maintain a constant chemical potential. In the final equilibrium state the concentrations of carbon and